Out-of-equilibrium quantum fields with conserved charge

D. J. Bedingham [*]

Centre for Theoretical Physics, University of Sussex,

Falmer, Brighton BN1 9QJ, U.K.

February 1, 2008

Abstract

We study the out-of-equilibrium evolution of an $O(2)$-invariant scalar field in which a conserved charge is stored. We apply a loop expansion of the 2-particle irreducible effective action to 3-loop order. Equations of motion are derived which conserve both total charge and total energy yet allow for the effects of scattering whereby charge and energy can transfer between modes. Working in $(1+1)$-dimensions we solve the equations of motion numerically for a system knocked out of equilibrium by a sudden temperature quench. We examine the initial stages of the charge and energy redistribution. This provides a basis from which we can understand the formation of Bose-Einstein condensates from first principles.

PACS numbers: 03.75.Nt, 11.30.Fs, 64.90.+b.

1   Introduction

The formation of a Bose-Einstein condensate involves a significant proportion of the total charge in a system relocating to occupy the lowest energy state. This is achieved experimentally using dilute atomic gases where the conserved charge corresponds to the total number of atoms and the condensate is formed by reducing the temperature of the gas using laser and evaporative cooling. We can understand Bose-Einstein condensation (BEC) by considering the equilibrium state of a bosonic gas [1, 2, 3, 4], but the question of precisely how the condensate arises as the gas responds to a change in its external conditions is a much more difficult problem (notable examples can be found in Refs.[5, 6, 7]). This process is a very-many-body problem encompassing the properties of cold, trapped atoms and importantly, interatomic interactions.

A theoretical understanding of condensate formation has recently been motivated by the possibility of observing the spontaneous formation of defects [8]. The vortices already observed in rotating condensates could form spontaneously if the cooling process were to happen quickly enough. The mechanism by which this occurs has consequences not only for condensed matter physics but also for cosmology where it is predicted that similar defects may have formed spontaneously in the early universe [9]. Experimental production of spontaneous defects in atomic gases would effectively allow us to test cosmological theories in the laboratory.

In this article we shall consider the initial stages of the dynamical process by which charge and energy is redistributed between modes following a sudden drop in the ambient temperature. Recent progress has been made towards understanding such equilibration processes of quantum fields in Refs.[10, 11, 12, 13, 14, 15]. In particular, the method of Refs.[10, 11, 13] uses the loop expansion for the 2-particle irreducible (2PI) effective action where thermalization is observed at 3-loop order [10]. Here we apply this method to a system containing a conserved finite charge.

In the next section we outline our method for a relativistic scalar field theory invariant under $O(2)$-transformations (the non-relativistic theory emerges for low temperatures as is demonstrated in [16]). This is one of the simplest models to have a conserved Noether charge, representing some

---

[*]email:d.j.bedingham@sussex.ac.uk

1

conserved quantum number. We derive equations of motion describing the evolution of the Green functions of the theory. In section 3 we consider the initial conditions needed to fully describe the system. For convenience we choose an initial equilibrium state. In section 4 we solve the equations of motion numerically. Due to computational constraints we work in one space and one time dimension. Though there is no phase transition in (1+1)-dimensions, trapped finite-size gases are known to exhibit interesting phenomena associated with a macroscopic occupation of the lowest energy state [4, 17]. Here we examine the initial stages of the charge and energy redistribution which must form the basis by which BEC occurs.

2 Dynamical equations

To describe out-of-equilibrium behavior we use the Schwinger-Keldysh technique [18, 19, 20]. Given an initial distribution of states with density operator $\hat{\rho}$ at time t_i, the expectation of an operator $\hat{\mathcal{O}}$ at some later time t is given in the Heisenberg picture by

$$\langle \hat{\mathcal{O}}(t) \rangle = \mathrm{Tr}\left\{ \hat{\rho}\hat{\mathcal{O}}(t) \right\}. \tag{1}$$

In the path-integral formulation, the time contour C begins at time t_i, evolves forward to time t, then returns to t_i.

We are interested in considering the response of a scalar field to a rapid drop in temperature. Assuming that the system is in equilibrium prior to the temperature quench, we may take the original equilibrium distribution as our initial distribution of states. Following the quench, as the system evolves with lower energy, it is forced to seek a new equilibrium.

Since our initial state has non-zero charge, the grand canonical ensemble provides the obvious choice of density operator. Given a Hamiltonian $\hat{H}$, charge $\hat{Q}$, initial temperature $T = 1/\beta$ and chemical potential μ, this is given by

$$\hat{\rho} = \exp\left\{ -\beta\left(\hat{H} - \mu\hat{Q}\right) \right\}. \tag{2}$$

We are free to adjust the effective parameters of $\hat{H}$ in order to fix our initial distribution. The initial conditions are considered in more detail in section 3.

The Hamiltonian density and charge operators for the self-interacting $O(2)$-invariant scalar theory are

$$\mathcal{H} = \frac{1}{2}\pi_a\pi_a + \frac{1}{2}\nabla\phi_a\nabla\phi_a + \frac{1}{2}m^2\phi_a\phi_a + \frac{\lambda}{4!}\left(\phi_a\phi_a\right)^2,$$
$$Q = \int \mathrm{d}x\left(\pi_1\phi_2 - \pi_2\phi_1\right), \tag{3}$$

where $a = 1, 2$ and repeated indices are summed over in the usual way. We proceed by writing out the Schwinger-Dyson equation for the 2-point Green function of this field [20] (we suppress field indices initially)

$$(\Box_x + m^2)G_2(xx_1) + \frac{\lambda}{6}G_4(xxxx_1) = -i\delta(x - x_1). \tag{4}$$

Diagrammatically, the 2-point Green function can be represented by a line as follows

$$G_2(x_1x_2) = x_1\!\bullet\!\!-\!\!\bullet\, x_2 \tag{5}$$

The 4-point Green function can then be written as a coupling expansion in terms of the 2-point Green function

$$G_4(x_1x_2x_3x_4) = \quad + \quad + \quad - i\lambda\int \mathrm{d}y \quad + \cdots. \tag{6}$$

2

Setting $x_2 = x_2 = x_3 = x$ we have

$$G_4(xxxx_1) = 3\ x\!\!\underset{}{\bigcirc}\!\!\!-\!\!\!-\bullet x_1\ -i\lambda\int dy\ x\!\!\overset{}{\underset{y}{\bigcirc}}\!\!\bullet x_1\ +\cdots. \tag{7}$$

The first term on the right-hand side results from disconnected 2-point Green functions. Truncating the series at this term constitutes a 'mean-field' linearization of Eq.(4), known as the Hartree approximation. Since we wish to incorporate scattering of particles with the movement of charge and energy between modes, it is crucial that we keep at least the $\mathcal{O}(\lambda)$ term in the series expansion. It seems clear when we look at Eq.(6) that the last term is necessary if we wish to see scattering effects.

Replacing field indices and neglecting the point-number label (all Green functions under consideration from now on are 2-point) we may rewrite the Schwinger-Dyson equation as

$$(\Box_x\delta_{ac} + M_{ac}^2(x))G_{cb}(x,y) + i\int_C dz\Sigma_{ac}(x,z)G_{cb}(z,y) = -i\delta_{ab}\delta_C(x-y), \tag{8}$$

where M is the effective mass and Σ is the non-local self-energy. Using the expansion of Eq.(7) and reinterpreting the algebraic form of the diagrams gives the effective mass as

$$M_{ab}^2(x) = m^2\delta_{ab} + \frac{\lambda}{6}\left[G_{cc}(x,x)\delta_{ab} + 2G_{ab}(x,x)\right], \tag{9}$$

and the non-local self-energy as

$$\Sigma_{ab}(x,y) = -2\left(\frac{\lambda}{6}\right)^2\left[G_{cd}(x,y)G_{cd}(x,y)G_{ab}(x,y) + 2G_{ac}(x,y)G_{db}(x,y)G_{dc}(x,y)\right]. \tag{10}$$

We began with the Schwinger-Dyson equation and performed a coupling expansion of the 4-point Green function. The above result is equivalently obtained by starting with the 2PI effective action and truncating at 3-loop order as is shown in Refs.[11, 13] (e.g. our Eq.(8) corresponds to Eq.(13) of Ref.[13]). In each of these references, a $1/N$ expansion is used in order to derive M and Σ. Although in principle our coupling expansion can be derived by truncating the $1/N$ expansion at $\mathcal{O}(\lambda^2)$, this would require working to NNLO in order to encounter the $\mathcal{O}(1/N^2)$ term on the right hand side of Eq.(10). The weak-coupling limit of the NLO approximation is briefly considered in Ref.[13].

The problem we face is to solve Eq.(8) for some given set of initial conditions. The 2-point Green functions represent a time-contour ordered product of field operators

$$G_{ab}(x,y) = \langle T_C\phi_a(x)\phi_b(y)\rangle. \tag{11}$$

The usual procedure for solving the Schwinger-Dyson equation is to decompose the Green functions as [20]

$$G_{ab}(x,y) = \theta_C(x_0 - y_0)G_{ab}^>(x,y) + \theta_C(y_0 - x_0)G_{ab}^<(x,y) \tag{12}$$

such that

$$\begin{aligned}
G_{ab}^>(x,y) &= \langle\phi_a(x)\phi_b(y)\rangle, \\
G_{ab}^<(x,y) &= \langle\phi_b(y)\phi_a(x)\rangle.
\end{aligned} \tag{13}$$

Now following the method outlined in Refs.[11, 13] we take real and imaginary parts

$$\begin{aligned}
F_{ab}(x,y) &= \frac{1}{2}\left[G_{ab}^>(x,y) + G_{ab}^<(x,y)\right] = \mathrm{Re}G_{ab}^>(x,y), \\
\rho_{ab}(x,y) &= i\left[G_{ab}^>(x,y) - G_{ab}^<(x,y)\right] = -2\mathrm{Im}G_{ab}^>(x,y).
\end{aligned} \tag{14}$$

The function ρ is the spectral function and F is the symmetric propagator.

Similarly, we perform a decomposition of the self-energy

$$\Sigma_{ab}(x,y) = \theta_C(x_0 - y_0)\Sigma_{ab}^{>}(x,y) + \theta_C(y_0 - x_0)\Sigma_{ab}^{<}(x,y), \tag{15}$$

and again take real and imaginary parts

$$
\begin{aligned}
\Sigma_{ab}^{F}(x,y) &= \frac{1}{2}\left[\Sigma_{ab}^{>}(x,y) + \Sigma_{ab}^{<}(x,y)\right], \\
\Sigma_{ab}^{\rho}(x,y) &= i\left[\Sigma_{ab}^{>}(x,y) - \Sigma_{ab}^{<}(x,y)\right].
\end{aligned} \tag{16}
$$

We can now reexpress the Schwinger-Dyson equation in terms of F and ρ (cf. Eqs.(70) and (71) in Ref.[13])

$$
\begin{aligned}
(\Box_x \delta_{ac} + M_{ac}^2)F_{cb}(x,y) &= -\int d\mathbf{z}\left\{\int_0^{x_0} dz_0 \Sigma_{ac}^{\rho}(x,z)F_{cb}(z,y) - \int_0^{y_0} dz_0 \Sigma_{ac}^{F}(x,z)\rho_{cb}(z,y)\right\}, \\
(\Box_x \delta_{ac} + M_{ac}^2)\rho_{cb}(x,y) &= -\int d\mathbf{z}\left\{\int_{y_0}^{x_0} dz_0 \Sigma_{ac}^{\rho}(x,z)\rho_{cb}(z,y)\right\},
\end{aligned} \tag{17}
$$

where now

$$M_{ab}^2(x) = m^2 \delta_{ab} + \frac{\lambda}{6}\left[F_{cc}(x,x)\delta_{ab} + 2F_{ab}(x,x)\right] \tag{18}$$

and

$$
\begin{aligned}
\Sigma_{ab}^{F} &= -2\left(\frac{\lambda}{6}\right)^2\left[\left(F_{cd}F_{cd} - \frac{1}{4}\rho_{cd}\rho_{cd}\right)F_{ab} - \frac{1}{2}F_{cd}\rho_{cd}\rho_{ab}\right.\\
&\qquad\left. +2\left(F_{ac}F_{db}F_{dc} - \frac{1}{4}F_{ac}\rho_{db}\rho_{dc} - \frac{1}{4}\rho_{ac}F_{db}\rho_{dc} - \frac{1}{4}\rho_{ac}\rho_{db}F_{dc}\right)\right], \\
\Sigma_{ab}^{\rho} &= -2\left(\frac{\lambda}{6}\right)^2\left[\left(F_{cd}F_{cd} - \frac{1}{4}\rho_{cd}\rho_{cd}\right)\rho_{ab} + 2F_{cd}\rho_{cd}F_{ab}\right.\\
&\qquad\left. +2\left(\rho_{ac}F_{db}F_{dc} + F_{ac}\rho_{db}F_{dc} + F_{ac}F_{db}\rho_{dc} - \frac{1}{4}\rho_{ac}\rho_{db}\rho_{dc}\right)\right].
\end{aligned} \tag{19}
$$

Before attempting to solve these equations, we express them in momentum space. In general, given that $\int_{\mathrm{p}} = \int d^d p/(2\pi)^d$, we can write

$$G(t_1,t_2;\mathbf{x}-\mathbf{y}) = \int_{\mathrm{p}} e^{i\mathbf{p}(\mathbf{x}-\mathbf{y})}G(t_1,t_2;\mathbf{p}) \tag{20}$$

due to spatial translation invariance. The self-energy terms Σ^F and Σ^{ρ} take the form given above but factors in each term have momentum values $\mathbf{p_1}$, $\mathbf{p_2}$ and $(\mathbf{p}-\mathbf{p_1}-\mathbf{p_2})$ respectively. Integrations are performed over $\mathbf{p_1}$ and $\mathbf{p_2}$ and the self-energy carries a momentum label $\mathbf{p}$.

The dynamical equations become

$$
\begin{aligned}
\left[(\partial_{t_1}^2 + \mathbf{p}^2)\delta_{ac} + M_{ac}^2(t_1)\right]F_{cb}(t_1,t_2;\mathbf{p}) &= -\left\{\int_0^{t_1} dt' \Sigma_{ac}^{\rho}(t_1,t';\mathbf{p})F_{cb}(t',t_2;\mathbf{p})\right.\\
&\qquad\left. -\int_0^{t_2} dt' \Sigma_{ac}^{F}(t_1,t';\mathbf{p})\rho_{cb}(t',t_2;\mathbf{p})\right\}, \\
\left[(\partial_{t_1}^2 + \mathbf{p}^2)\delta_{ac} + M_{ac}^2(t_1)\right]\rho_{cb}(t_1,t_2;\mathbf{p}) &= -\left\{\int_{t_2}^{t_1} dt' \Sigma_{ac}^{\rho}(t_1,t';\mathbf{p})\rho_{cb}(t',t_2;\mathbf{p})\right\},
\end{aligned} \tag{21}
$$

where the effective mass squared, expressed in the momentum basis is

$$M_{ab}^2(t) = m^2 \delta_{ab} + \frac{\lambda}{6}\left[\int_{\mathrm{p}} F_{cc}(t,t;\mathbf{p})\delta_{ab} + 2\int_{\mathrm{p}} F_{ab}(t,t;\mathbf{p})\right]. \tag{22}$$

4

It remains to solve these equations for some given set of initial conditions. Since our equations involve a weak-coupling expansion we should be careful to note that they are likely to give inaccurate answers should the coupling corrections become large. For this reason we should not stray too far from equilibrium.

Finally, by taking expectations of the Hamiltonian and charge operators and substituting from Eq.(7) for the 4-point Green function, we find the overall energy is given by

$$
\begin{aligned}
E &= \int_{\mathrm{p}} E_{\mathrm{p}}(t) \\
&= \frac{1}{2} \int_{\mathrm{p}} \left\{ [\partial_t \partial_{t'} F_{aa}(t, t'; \mathbf{p})]_{t=t'=0} + \left(\mathbf{p}^2 + m^2 + \frac{\lambda}{24} \int_{\mathrm{p'}} F_{cc}(t, t; \mathbf{p'}) \right) F_{aa}(t, t; \mathbf{p}) \right. \\
&\quad + \left(\frac{\lambda}{12} \int_{\mathrm{p'}} F_{ac}(t, t; \mathbf{p'}) \right) F_{ca}(t, t; \mathbf{p}) \\
&\quad \left. + \frac{1}{2} \int_0^t \mathrm{d}t' \left(\Sigma_{ac}^\rho(t, t'; \mathbf{p}) F_{ca}(t', t; \mathbf{p}) - \Sigma_{ac}^F(t, t'; \mathbf{p}) \rho_{ca}(t', t; \mathbf{p}) \right) \right\}
\end{aligned}
\tag{23}
$$

and the overall charge is given by

$$
Q = \int_{\mathrm{p}} Q_{\mathrm{p}}(t) = \int_{\mathrm{p}} [\partial_t F_{12}(t, t'; \mathbf{p}) - \partial_t F_{21}(t, t'; \mathbf{p})]_{t=t'}.
\tag{24}
$$

Each of these quantities can be shown both analytically and numerically to be conserved by the dynamical equations. However, charge and energy are indeed capable of exchange between modes.

3 Initial Conditions

The Schwinger-Dyson equations embody not only Heisenbergs equation of motion for the field but also the equal time commutation relations (ETCR). It should come as no surprise that the ETCR are conserved by our dynamics so long as they are enforced by the initial conditions. The ETCR for our model are

$$
[\phi_a(\mathbf{x}, t), \pi_b(\mathbf{y}, t)] = i\delta_{ab}\delta(\mathbf{x} - \mathbf{y}),
$$
$$
[\phi_a(\mathbf{x}, t), \phi_b(\mathbf{y}, t)] = [\pi_a(\mathbf{x}, t), \pi_b(\mathbf{y}, t)] = 0.
\tag{25}
$$

These translate into statements about the spectral function

$$
[\partial_t \rho_{ab}(t, t'; \mathbf{p})]_{t=t'} = \delta_{ab},
$$
$$
\rho_{ab}(t, t; \mathbf{p}) = [\partial_t \partial_{t'} \rho_{ab}(t, t'; \mathbf{p})]_{t=t'} = 0.
\tag{26}
$$

The ETCR are not sufficient to constrain the initial conditions. Other symmetry requirements which derive from the spectral function and symmetric propagator definitions Eq.(14) must also be satisfied

$$
F_{ab}(t_1, t_2; \mathbf{p}) = F_{ba}(t_2, t_1; \mathbf{p}),
$$
$$
\rho_{ab}(t_1, t_2; \mathbf{p}) = -\rho_{ba}(t_2, t_1; \mathbf{p}).
\tag{27}
$$

(It can be checked that if these conditions are satisfied initially, then the dynamical equations preserve them for all later times.) Having satisfied the quantum commutation relations and other symmetry requirements, it remains to chose the initial conditions for these unspecified functions. Here we shall choose free field equilibrium values for some given temperature $T = 1/\beta$, and chemical potential μ. Setting the initial time $t_i = 0$ we have

$$
F_{12}(0, 0; \mathbf{p}) = F_{21}(0, 0; \mathbf{p}) = 0,
$$

$$F_{11}(0, 0; \mathbf{p}) = F_{22}(0, 0; \mathbf{p}) = \frac{1}{2\omega} \left[\frac{1}{e^{\beta(\omega-\mu)} - 1} + \frac{1}{e^{\beta(\omega+\mu)} - 1} + 1 \right],$$

$$[\partial_t F_{11}(t, 0; \mathbf{p})]_{t=0} = [\partial_t F_{22}(t, 0; \mathbf{p})]_{t=0} = 0,$$

$$[\partial_t F_{12}(t, 0; \mathbf{p})]_{t=0} = -[\partial_t F_{21}(t, 0; \mathbf{p})]_{t=0} = \frac{1}{2} \left[\frac{1}{e^{\beta(\omega-\mu)} - 1} - \frac{1}{e^{\beta(\omega+\mu)} - 1} \right],$$

$$[\partial_t \partial_{t'} F_{ab}(t, t'; \mathbf{p})]_{t=t'=0} = \omega^2 F_{ab}(0, 0; \mathbf{p}), \tag{28}$$

where $\omega = \sqrt{\mathbf{p}^2 + M_0^2}$, and M_0^2 can be viewed as the effective mass squared prior to the temperature quench.

Referring to Eq.(24), the overall charge is given by

$$Q = \int_{\mathrm{p}} \left[\frac{1}{e^{\beta(\omega-\mu)} - 1} - \frac{1}{e^{\beta(\omega+\mu)} - 1} \right]. \tag{29}$$

This value is conserved throughout the subsequent evolution of Green functions.

4   Numerical results

In this section we present our numerical solutions to Eqs. (21).

Eqs. (21) are integro-differential equations for F_{ab} and ρ_{ab}, each of which are functions of t_1, t_2 and $\mathbf{p}$. The equations involve coefficients which are themselves dependent on $F_{ab}(t, t'; \mathbf{p})$ and $\rho_{ab}(t, t'; \mathbf{p})$ for t and t' up to and including t_1 and t_2, and for all values of $\mathbf{p}$. The right hand side of Eqs (21) involve two integrations over internal momenta and one time integration. In addition these integrations must be performed for all external values of t_1, t_2 and $\mathbf{p}$. In light of this it would be computationally unfeasible to work in any greater than (1+1)-dimensions. Also, the range of the time integrations becomes greater as t_1 and t_2 become greater and contrives to slow the calculations down at later times. This limits us to considering only early times.

The (1+1)-dimensional continuum is replaced by a spatially periodic lattice. Integrations are performed by converting into discrete sums

$$\int \frac{\mathrm{d}\mathbf{p}}{2\pi} \rightarrow \frac{1}{Na} \sum_{n=1}^{N}. \tag{30}$$

N is the number of lattice points, a is the spatial lattice spacing, and $Na = L$ is the length of the spatial dimension . Differential equations are solved by a basic leapfrog method. The time step h in units of $1/M_{\mathrm{INIT}}$ is chosen to be 0.1 where M_{INIT} is the initial value of the effective mass following the quench. A corresponding choice of $a = 0.4/M_{\mathrm{INIT}}$ gives stability with $h/a = 0.25$. Choosing $N = 100$ we have a lattice size $L = 40$ in units of $1/M_{\mathrm{INIT}}$. With periodic boundary conditions the momenta are given by

$$\mathbf{p}^2 \rightarrow -\frac{2}{a^2} \left(\cos \frac{2\pi n}{N} - 1 \right). \tag{31}$$

Although these elementary techniques may provide a relatively poor approximation to the continuum, they are fast and provide stable results. Also, the conservation of energy, charge and other symmetries are transparent upon considering a single iteration of the dynamical process.

Other parameters are chosen in units of M_{INIT} as $T = 10$, $\mu = 0.1$ and $M_0 = 4$. These correspond to a total energy of 172.92 and a total charge of 1.84. These values have no particular significance, they are chosen simply to represent the general behavior. Larger values of M_0 provide a greater impulse, knocking the system further from equilibrium. Larger values of T reduce the impact of changing the mass parameter on the charge and energy distributions. The chemical potential must be less than M_0. For (3+1)-dimensional systems, the closer μ is to M_0, the closer the system is to the critical point. The coupling $\lambda = 0.5$ is small in order to make sense of a coupling expansion yet large enough to see appreciable scattering effects relatively quickly.
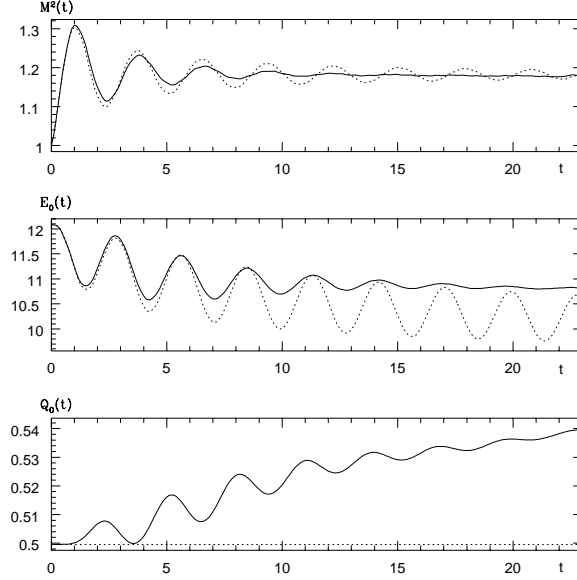
Figure 1: Evolution of effective mass squared, energy in the lowest mode, and charge in the lowest mode. The dashed line is the Hartree approximation, the solid line is the current approximation.

Fig.1 shows plots with the effective mass squared $M^2(t)$ (Eq.(22)), the energy in the lowest mode $E_0(t)$ (see Eq.(23)), and the charge in the lowest mode $Q_0(t)$ (see Eq.(24)). The dashed line is the Hartree or mean-field approximation for comparison. In the Hartree approximation only terms of order λ are kept in the dynamical equations. Solid lines represent solutions to Eqs.(21). An important feature to observe is that the charge in the lowest energy state is constant in the Hartree approximation but is free to change at next order in λ where scattering effects are incorporated. Oscillations in $M^2(t)$ and $E_0(t)$ are damped out more effectively in the higher order calculation.

Fig.2 shows the evolution of the symmetric propagator with time. For $F_{11}(t,t;0)(= F_{22}(t,t;0))$ we observe a much more effective damping of oscillations than in the Hartree approximation. We also observe an oscillatory decrease in correlations between the field at time t and the field at time 0. This indicates that the system is moving towards some final outcome which is independent of the initial conditions and dependent only on the conserved quantities which characterize the system. It should be noted that the equations of motion may be reversed in time and initial conditions can always be recovered. A fixed point equilibrium solution in the future can in principle be approached arbitrarily closely but never reached [11]. There is zero equal time correlation between fields ϕ_1 and ϕ_2.

Fig.3 shows the distribution of charge in the different momentum modes (Eq.(24)). The upper figure indicates the initial charge distribution (see Eq.(29)). The lower momentum modes store a greater amount of charge. As the system evolves we see that charge moves out-of the region $p > 1$ and into the region $p < 1$. The change in charge at each momentum value is shown at times 0, 10, and 20. This process fits our intuition where we would expect that charge moves into the lower energy states as the temperature decreases.

The energy distribution of Eq.(23) is given in Fig.4. The upper figure gives the initial energy distribution. In the continuum we would expect the energy to increase quadratically with p and without bound. Our lattice approximation flattens out the energy spectrum at the upper limit of momentum whilst the spectrum is approximately quadratic at low momenta. Following the quench we see a movement of the energy from the region $p < 1$ into the region $p > 1$. The change in the energy distribution becomes less oscillatory as time increases. This is a reflection of the
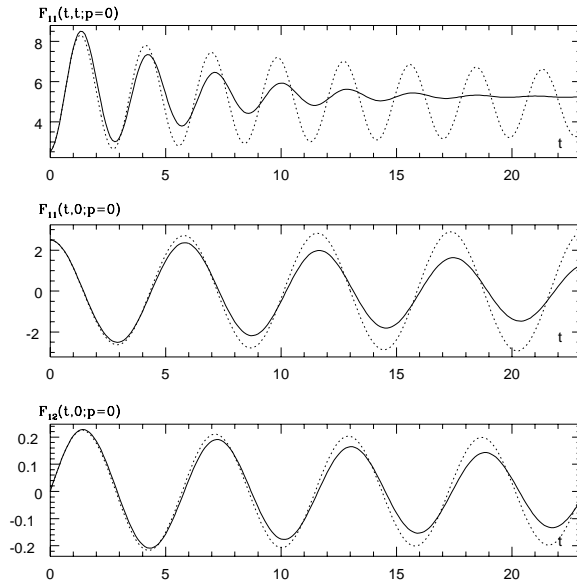
Figure 2: Evolution of the symmetric propagator. The dashed line is the Hartree approximation, the solid line is the current approximation.

fact that oscillations in both the effective mass and the equal time propagator are damped out as time increases.

Fig.5 displays the increase in spatial correlations as a result of the drop in temperature. The correlation function

$$F_{11}(t,t;\mathbf{x}) = \int_{\mathbf{p}} e^{i\mathbf{p}\mathbf{x}} F_{11}(t,t;\mathbf{p}) \tag{32}$$

shows a growth in amplitude and a growth in the size of the region in which the field is correlated. These regions can be interpreted as domains in which the field has strong correlations [21]. The rate at which these domains grow has consequences for the formation of defects in higher dimensional systems undergoing a symmetry breaking phase transition [22]. In our simulations it is found that the correlation function quickly grows to a new stable function which then remains approximately constant.

In addition, in our numerics we observe conservation of total charge, conservation of total energy, and conservation of commutation relations.

5 Conclusions

We have considered the quantum field dynamics of an $O(2)$-invariant scalar field theory with a conserved charge. We have argued that in deriving our equations of motion, it is crucial that we work to at least 3-loop order in the 2-particle irreducible effective action. This is the lowest order at which the effects of scattering are included, allowing for the movement of charge between modes. In lower order calculations, the charge in each mode is artificially confined to that mode. Since BEC is essentially characterized by the charge distribution, in order to consider the formation process, the charge in the system must be able to redistribute in response to some external stimulus. More generally, to understand any equilibration process involving finite conserved charge we must account for the transfer of charge between modes.

We have considered a (1+1)-dimensional system. Although this does not allow us to model a condensation process, we are able to examine the charge and energy distributions as they evolve in time. For a sudden drop in temperature modelled by a sudden change in the effective mass
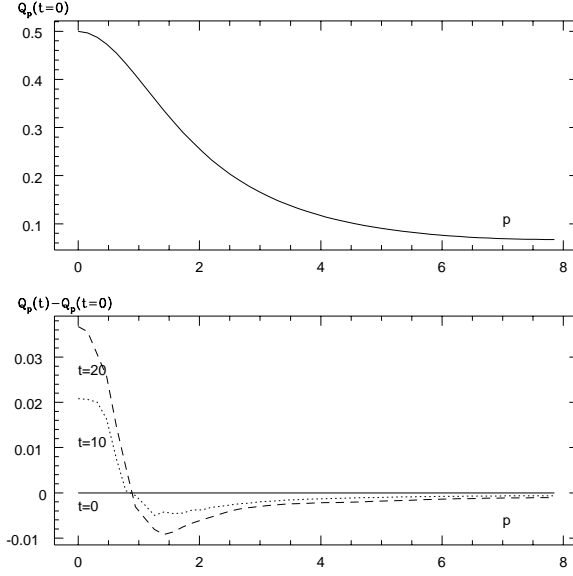
Figure 3: Charge distributions at a series of times.

squared, we observe an expected general movement of charge from higher to lower momentum modes. This is accompanied by a movement of energy from lower to higher momentum modes.

A (3+1)-dimensional version of this calculation remains a desirable goal for the future. An improvement of the algorithm in order to run the calculation to much later times would also be welcome.

Acknowledgements

References

[1] H. E. Haber and H. A. Weldon, Phys. Rev. **D25**, 502 (1982).

[2] J. I. Kapusta, Phys. Rev. **D24** 426 (1981).

[3] K. M. Benson, J. Bernstein, and S. Dodelson, Phys. Rev. **D44** 2480 (1991).

[4] F. Dalfovo and S. Giorgini, Rev. Mod. Phys. **71** 463 (1999).

[5] H. T. C. Stoof, Phys. Rev. Lett. **66** 3148 (1991).

[6] H. T. C. Stoof, Phys. Rev. **A45** 8398 (1992).

[7] M. D. Lee and C. W. Gardiner, Phys. Rev. **A62**, 033606 (2000).

[8] J. R. Anglin and W. H. Zurek, Phys. Rev. Lett. **83** 1707 (1999).

[9] T. W. B. Kibble, J. Phys. **A9**, 1387 (1976).

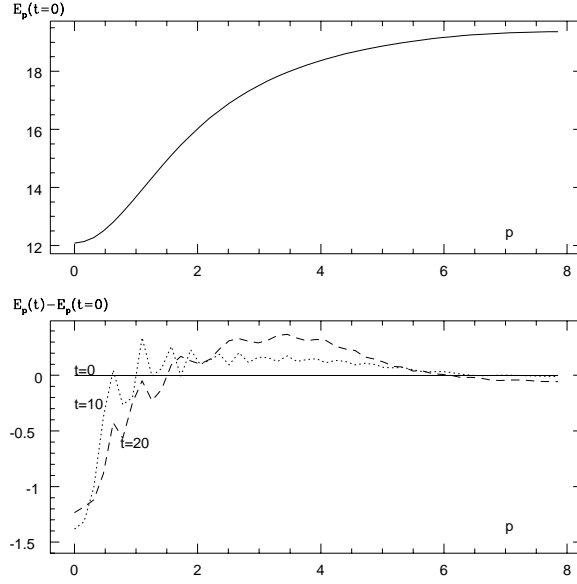[10] J. Berges and J. Cox, Phys. Lett. **B517**, 369 (2001).

Figure 4: Energy distributions at a series of times.

[11] J. Berges, Nucl. Phys. **A699**, 847 (2002).

[12] G. Aarts and J. Smit, Phys. Rev. **D61**, 025002 (2000).

[13] G. Aarts *et al.*, Phys. Rev. **D66**, 045008 (2002).

[14] L. M. A. Bettencourt and C. Wetterich, Phys. Lett. **B430**, 140 (1998).

[15] J. Baacke and A. Heinen, Phys. Rev. **D67**, 105020 (2003).

[16] T. S. Evans, hep-ph/9510298.

[17] K. Kirsten and D. J. Toms, Phys. Lett. **B 368**, 119 (1996).

[18] J. Schwinger, J. Math. Phys. 2, 407 (1961).

[19] L. V. Keldish, Sov. Phys. JETP 20, 1018 (1965).

[20] N. P. Landsman and Ch. G. van Weert, Phys. Rep. **145**, 141 (1987).

[21] D. Boyanovsky, D.-S. Lee and A. Singh, Phys. Rev. **D 48**, 800 (1993).
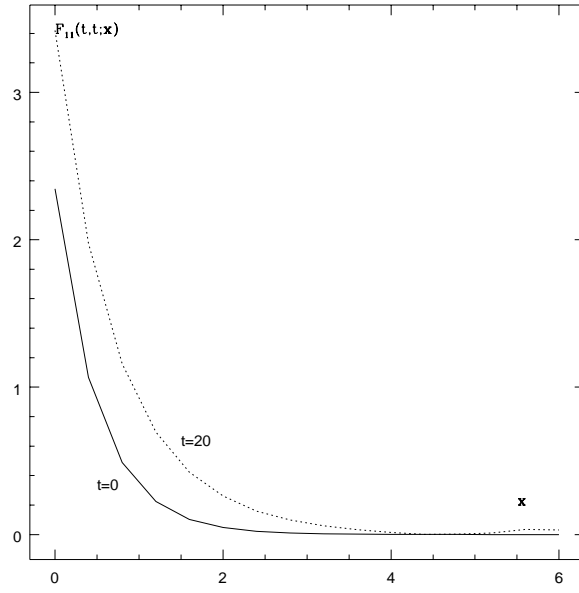
[22] W. H. Zurek, Nature **317**, 505 (1985).

Figure 5: Changes in the spatial correlation function with time.